On the Computations of Specific Surface Area and Specific Grain Contact Area from Snow 3D Images

Frederic Flin[1,*], Bernard Lesaffre[1], Anne Dufour[1], Luc Gillibert[1], Alsidqi Hasan[1], Sabine Rolland du Roscoat[2], Simon Cabanes[1], Philippe Pugliese[1]

[1]Centre d'Etudes de la Neige, CNRM - GAME URA 1357, Meteo-France - CNRS, 38400 Saint Martin d'Heres, France, [2]Laboratoire 3SR UMR 5521, CNRS - INPG - UJF, 38041 Grenoble cedex 9, France

* Corresponding author. E-mail: frederic.flin@meteo.fr

Estimating the Specific Surface Area (SSA) of snow and firn using three-dimensional (3D) images is now widely used in the snow and ice community. However, little information is available about parameters that may impact the final quantitative measurements. In particular, important questions such as the accuracy of the numerical methods used, the possible limitations due to image resolution or the minimal Representative Elementary Volume (REV) for this particular quantity remain.
To try to fill in the gap, we investigated different features of the numerical SSA measurement from 3D images. We obtained the principal following results: 1) the main standard SSA numerical approaches provide globally similar results. However, each method has its own inherent drawbacks: the stereological approach[1-2] does not handle anisotropic structures properly, the marching cubes[3] tends to overestimate the surface and the voxel projection method[4] is more highly sensitive to image resolution. 2) The resolution limit strongly depends on the numerical method and on the snow type. 3) The REV seems to be attained with a cube of 2.5 mm edge for all of the studied samples.
Based on a recently developed grain segmentation algorithm[5], a new SSA-related numerical estimator was defined and applied to snow samples: it provides an estimation of the Specific Grain Contact Area (SGCA), which seems a promising parameter to describe snow microstructure, e.g. to forecast the SSA that can be released by mechanical processing (neck breaking). The present study showed that the proportion of SGCA is particularly high for aged snow types. The results obtained provide a more comprehensive insight on the microtomographic approach and can be useful as well for snow modeling or other SSA measurement methods.

1. INTRODUCTION

Recently, the Specific Surface Area (SSA) has gained significant interest for the modeling of the physical and chemical behavior of snow[6]. Among all the existing methods devoted to SSA measurements, NIR approaches (see e.g.[7]) are probably the most effective and field-compliant techniques. However, these techniques often require approximations on the snow geometry or calibrations from other kinds of measurements.

Like methane adsorption[8], X-ray microtomography combined to image analysis is an appropriate means to provide the SSA of snow samples[9]. If the validity of the X-ray microtomography method has already been ascertained[10], some questions concerning its use remain:

1) What is the best numerical method to estimate the SSA? To our knowledge, three different approaches are commonly used to quantify the area of the ice-pore interface from three-dimensional (3D) images: the STereological approach[1-2] (ST), the Marching Cubes approach[3] (MC), and the voxel projection approach[4] (VP). However, no systematic comparisons have been done to check these methods for snow SSA estimations, in particular in terms of sensitivity to diverse parameters such as snow type or image resolution.

2) Concerning resolution, is there a minimal voxel size that ensures a realistic determination of the SSA? Based on experimental comparison with methane adsorption, Kerbrat et al.[10] propose 30 μm as a reasonable limit. However, some details

Physics and Chemistry of Ice 2010
Edited by Y. Furukawa, G. Sazaki, T. Uchida, N. Watanabe
Hokkaido University Press, 2011, Sapporo

of the surface may not be detectable at such a resolution, in particular for fresh snow.

3) What is the minimal Representative Elementary Volume (REV) for snow SSA and is it particulary sensitive to snow type? To our knowledge, since the first SSA estimations on snow using tomography[9, 11], the SSA REV has never been assessed on snow samples.

4) Can the tomographic approach provide SSA improved measurements that help in a better understanding of the snow microstructure? In particular, Voitkovsky et al.[12] have demonstrated that the specific grain contact surface is a parameter that is strongly correlated with the snow mechanical properties. Due to the recent development of grain segmentation algorithms[5, 13], an estimation of the Specific Grain Contact Area (SGCA) from 3D images seems now accessible.

Based on a large set of diverse tomographic images, this work proposes to answer all these questions by providing systematic numerical investigations on the impact of various parameters on the SSA estimation. It also presents a numerical method to compute the SGCA as well as a first practical application of this parameter. After presenting the images and methods that have been used in this study, we will focus on the main results obtained and their analyses.

2. MATERIALS AND METHODS

2.1. Image acquisition

The numerical tests were applied to various categories of tomographic images (see Table 1 for a brief summary): a first series of samples I01, I08 and I23 were obtained under controlled isothermal conditions in a cold room and correspond to Figures 5a, 5b and 5c of the paper given in reference 9. Two neighboring volumes were obtained under a controlled Temperature Gradient (TG) of 16K/m as described in a previous work[14]: E01 and E02 correspond to the same physical sample as depicted in Figure 3 of reference 14. Samples P03, P04 and P10 where taken at increasing depths in the natural snowpack of the Girose glacier (Ecrins, French Alps) during a field campaign on the 17th April 2009[15]. Finally, wet grains samples H03 and H05 where obtained by coarsening of water-saturated snow using a similar method to that of Raymond and Tusima[16]. After 48 and 142 h of growth respectively, the samples were drained out from their liquid water, filled with liquid 1-chloronaphtalhene around -1°C and frozen at –25°C before further machining. Small cores 9 mm in diameter were then extracted with precision hole-saw, sealed inside thin PMMA boxes and kept for tomography acquisition.

3D images of I and E series were obtained at the ID19 beamline of the European Synchrotron Radiation Facility (ESRF), while the series P and H were acquired with a cone beam tomograph (3SR Laboratory). In both cases, a specifically designed refrigerated cell was used, and the gray-level images obtained were contoured using a semi-automatic procedure. Finally, cubes of 512^3 voxels were extracted from the reconstructed 3D binary images.

Sample #	Voxel size (µm)	Snow type	Remarks
I01	4.91	PP/DF	Sampled 15 h after the snowfall[9]
I08	4.91	DF	Sampled 470 h after the snowfall[9]
I23	4.91	RG	Sampled 2026 h after the snowfall[9]
E01	4.91	FC/DH	3 weeks with TG = 16 K/m[14] downer volume
E02	4.91	FC/DH	3 weeks with TG = 16 K/m[14] upper volume
P03	8.48	PP/DF	Field, Girose glacier[15], 0.2 m depth
P04	8.59	PP/DF	Field, Girose glacier[15], 0.4 m depth
P10	6.10	RG	Field, Girose glacier[15], 1.6 m depth
H03	8.61	MF	Grain coarsening of water-saturated snow[16] and drainage after 48h
H05	8.59	MF	Grain coarsening of water-saturated snow[16] and drainage after 142h

Table 1. List of the diverse original snow samples studied in the present work. Snow type is defined according to the *International Classification for Seasonal Snow on the Ground*[17]: PP, Precipitation Particles; DF, Decomposing and Fragmented precipitation particles; RG, Rounded Grains; FC, Facetted Crystals; DH, Depth Hoar; MF, Melt Forms.

2.2. Quantitative Analysis

Three methods that are commonly used to compute the SSA from 3D images were compared:

1) The 3D version of the STereological approach[1-2] (ST): the method consists in averaging over the whole volume, the number of interface points per unit length on a linear path along the x, y or z directions. This method, as it is only valid for isotropic microstructures, is not particularly suited to snow, which is an anisotropic medium. However, SSA estimations computed on the supposed principal axes gives a reasonable reference to compare with other methods.

2) The Marching Cubes approach[3-4, 18] (MC): like any other triangulation technique, it consists in building a triangulated surface that globally fits the contours of the considered digital surface. Summing the area contributions of all the triangles provides the surface area of the whole image, and hence, its SSA. We presently used an implementation of this triangulation method available in the open-source software "Paraview" (http://www.paraview.org/).

3) The Voxel Projection (VP) method is based on a precise surface normal determination in order to estimate the area contribution of each voxel of the surface. Summing all the contributions of the interface gives a good estimation of the total surface[4, 19].

These three methods were tested on diverse snow types and image resolutions: for each sample, we computed the SSA estimations at the resolution of the original image, then increased the voxel size of the contoured binary images by a factor two. Each time we doubled the voxel size, we obtained a new SSA estimation, thus providing a means to check the resolution sensitivity of SSA estimation with 3D imaging.

It should be noted that increasing the voxel size by a factor two may lead to a threshold indetermination if exactly half of the subvoxels belong to a particular phase (ice or pore). To overcome this problem, two threshold images, including or excluding the undetermined voxels in the ice phase, were generated for a particular resolution. The final SSA was then estimated by averaging the SSA values obtained from the slightly different images.

In order to check the representativeness of the estimated SSA, values were computed in cubic neighborhoods growing from the center of the original high-resolution image. This test was only realized for the VP algorithm, as REV has no particular reason to depend on the estimation method.

Finally, we tried to estimate the SGCA for each of our snow image. For this purpose, we applied the recently-developed Curvature-Driven Grain Segmentation (CDGS) algorithm[5] that is based on a surface curvature analysis to propose a volume segmentation of the microstructure into geometrical grains. This method, which has been validated[5] on large wet grains by Diffraction Contrast Tomography[20-21] can be used directly to compute the SGCA. By defining SSA_{tot} as being the average of all the SSA contributions of the geometrical grains taken separately, we have:

$$SSA_{tot} = surface_{tot}/mass_{tot} \qquad (1)$$

As the ice masses defining SSA, SSA_{tot} and SGCA are exactly the same, we have the simple following relationship:

$$SSA_{tot} = SSA + SGCA \qquad (2)$$

Computing the SSA for each grain taken separately leads directly to SSA_{tot}. As the common SSA can easily be computed for the same snow image, the SGCA can directly be obtained from equation (2).

All computations presented in this article have been realized using a common laptop computer (DELL Latitude D630, Intel Core 2 Duo CPU 2GHz, RAM of 2 GB, 32-bit system). For computational time and memory reasons, all SSA estimations related to SGCA measurements were operated at a slightly decreased resolution: the voxel size of the 3D images was increased by a factor of two in the three axes.

3. RESULTS AND DISCUSSION

3.1. SSA Estimators and Voxel Size

The results concerning the sensitivity tests of the SSA numerical estimators are presented in Figures 1 and 2. The stereological method is depicted in the legends by the suffixes x, y, z, which represent the computation direction of the intercepts. The Marching Cubes and Voxel Projection methods can

be identified by the MC and VP suffixes, respectively. From these four graphs, a large variety of observations can be made:

1) At the smallest voxel size (between 4.91 and 6.10 μm), all the methods give similar results within a margin of about ±10 to 15%.

2) Excepting for the P03 and P10 images, the MC method systematically provides a higher SSA value than any other method. This is due to the method itself: to build a triangulated surface, the MC only takes into account the configuration of 8 neighboring voxels. As a result, slightly tilted digital planes are processed by the algorithm as series of steps, leading to a systematic overestimation of the triangulated surface. Diverse methods have been developed to overcome this problem (e.g. use of gray levels or smoothing), but these may create other artifacts depending on the image considered, such as systematic underestimation of the surface (see e.g. reference 9). Other triangulation methods than MC-based methods exist and may be more suitable to estimate SSA (see e.g the work of Glantz and Hilpert[22]).

3) The ST methods show a noticeable scatter in the results obtained between the vertical and horizontal directions. This is due to the inherent anisotropic nature of snow and firn microstructures[9, 11, 23]. This method has however the particular advantage to be weakly sensitive to the resolution decrease.

4) The VP method is however significantly impacted by the image resolution. This can be explained by the fact that it requires a precise estimation of the normal vectors on the ice-pore interface: a relatively high number of voxels are necessary to describe a particular detail of the image. When the resolution requirement is fulfilled (all samples excepting I01 and P03), this method gives results that are in perfect accordance with the stereological method.

5) The minimal acceptable image resolution to compute the SSA depends not only on the estimation method used, but also strongly on the snow type: from Figures 1 and 2, the SSA of coarse wet grains (sample H5) can reasonably be estimated with a voxel size of 120 μm. However, depending on the desired level of accuracy, the SSA estimated for very recent snow (samples I01 and P03) should be handled with care - even at a voxel size of 4.91 μm - for any method: the curves are steep enough to suggest that the SSA result would be slightly higher if the image was available at a better resolution. These numerical computations are in relatively good agreement with Kerbrat et al.'s conclusions[10] stipulating that the ice surface in alpine snowpack is essentially smooth up to a scale of 30 μm, but give a more detailed and contrasted picture of the involved phenomena. In particular, they show that the minimal acceptable resolution strongly depends on the SSA estimator and the snow type.

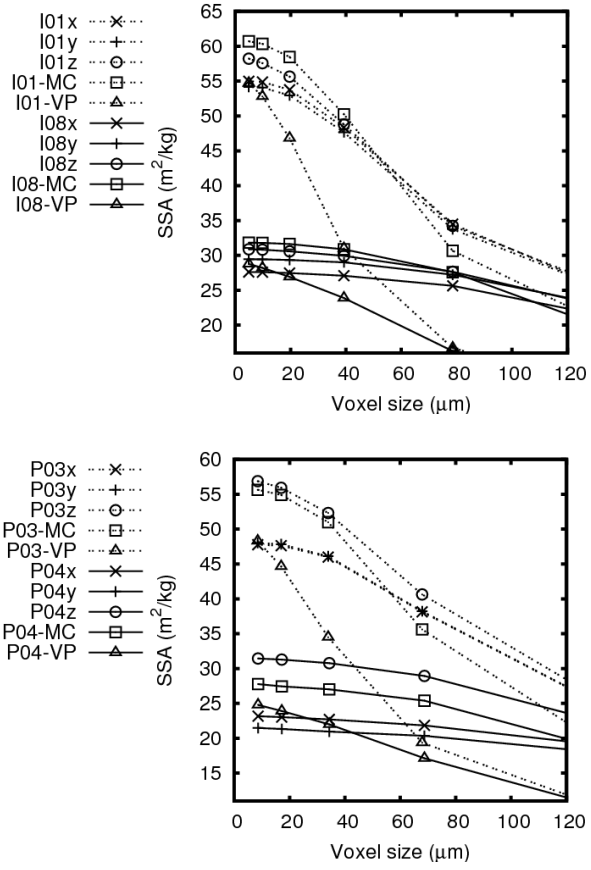

Figure 1. Evolution of the SSA with the voxel size for diverse estimation methods. Recent snow samples (PP/DF).

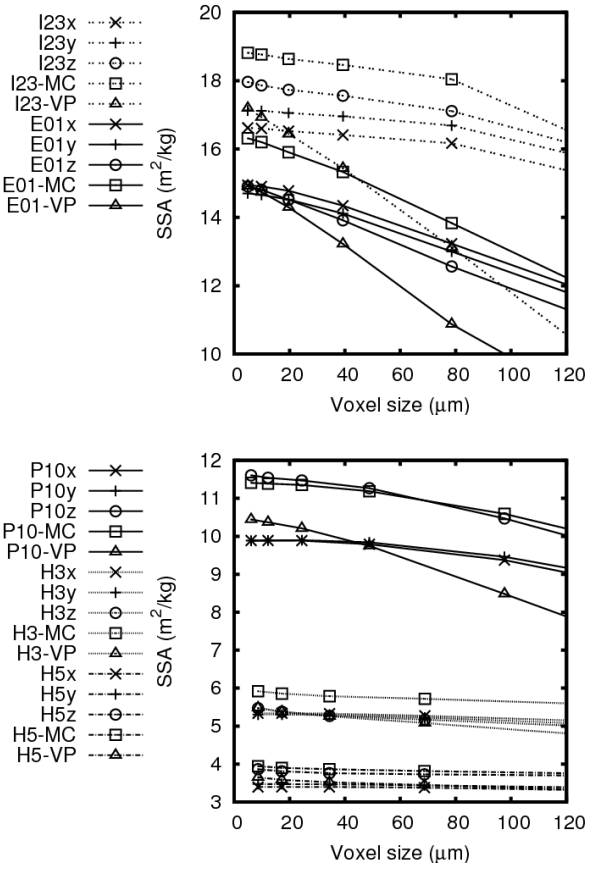

Figure 2. Evolution of the SSA with the voxel size for diverse estimation methods. Aged snow samples (RG, FC/DH, MF). Results obtained for the specimen E02 are very close from those obtained from specimen E01 and are not plotted on the graphs for a sake of legibility.

In summary, there is no ideal method to compute SSA: ST is particularly simple to implement, and robust in terms of image resolution decrease, but suffers from anisotropy effects. MC is more suited to process anisotropic images and is not too sensitive to resolution decrease. However, it constantly overestimates the real SSA, at least with the simplest implemented versions. VP is accurate and not sensitive to anisotropy effects. It is however particularly sensitive to resolution decrease: it should be dedicated to images whose resolution is significantly higher than the minimal useable resolution. When the image resolution available is low compared to the snow physical details, the best option would probably consist of using the mean of the intercepts in the three space directions (for both theoretical and empirical reasons, the z axis generally corresponds to a principal axis, and both of the x and y directions give very close results). While it neglects the possible horizontal heterogeneity of the studied sample, the recent technique proposed by Matzl and Schneebeli[24], may also be used to solve the problem.

3.2. Representative Elementary Volume

For most of the samples, the REV seems to be attained with a sufficient precision before the side of the image cube reaches 2.5 mm (see Figure 3). However, some samples (I01, E01-2, H5…) would probably benefit from a larger computation volume. In particular, it should be noticed that the E01 and E02 images, which were extracted from the same original sample differ by about 8% for a cubic neighborhood of 2.5 mm size. This REV error is slightly lower than the accuracy of the SSA methane adsorption method[8, 10].

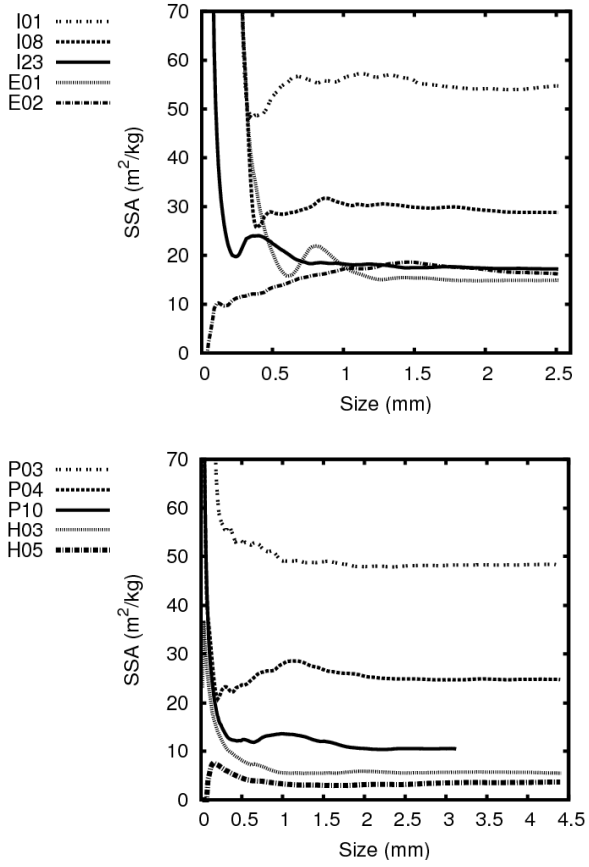

Figure 3. Evolution of the SSA with the edge size of the image for diverse snow samples.

3.3 Grain segmentation

Figures 4 and 5 provide the results of the CDGS algorithm obtained for two different samples. By checking the snapshots in detail, one may find locally some over or under-segmentations. However, based on previous comparisons with DCT on wet grains samples[5, 21], we think that the segmentation process is globally accurate and that applying the VP estimator to each of the grains identified gives reasonable estimations of the SGCA.

The results of the SGCA computations are plotted in Figure 6 for all the studied snow samples. Computations for I01 and I03 need to be considered as raw estimates, as these images are clearly underestimating the SSA of about 10% at the considered resolution (see 3.1).

From the Figure, the lower the SSA, the higher is the SGCA contribution in terms of % of SSA_{tot}. This means that aged snow samples (characterized with low SSA) can release a significant proportion of their Specific Surface Area by neck breaking.

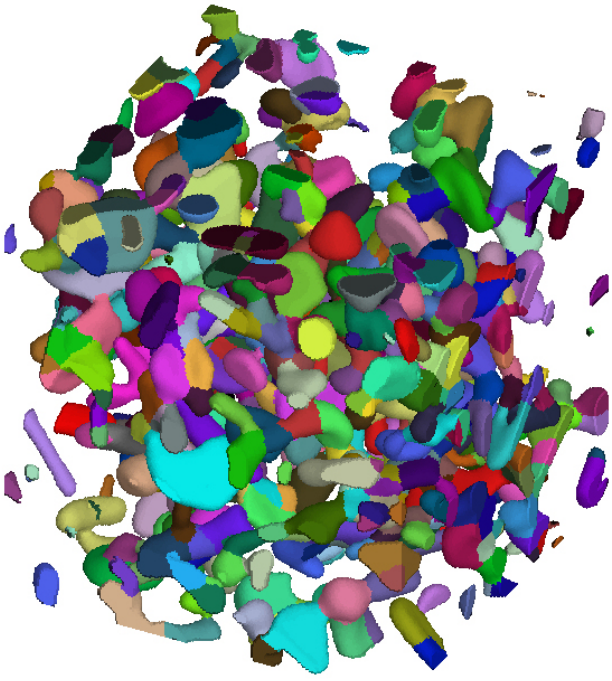

Figure 4. Rendering of sample I08 after applying the CDGS algorithm: each color level corresponds to a particular geometrical grain. Edge size: 256 voxels (~2.5 mm).

Figure 5. Rendering of sample H05 after applying the CDGS algorithm: each color level corresponds to a particular geometrical grain. Edge size: 256 voxels (~4.4 mm).

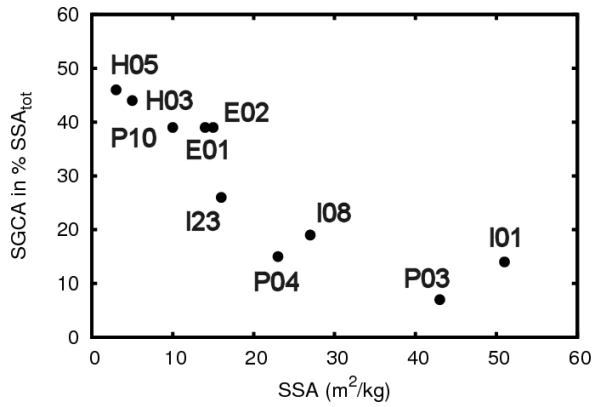

Figure 6. Dependence of the SGCA (in % of SSA_{tot}) with the SSA for all the snow samples considered in this study.

From a practical sampling point of view, these results may have interesting outcomes. They explain the differences that are sometime observed before and after mechanical processing (see e.g. the paragraph 21 of the work of Legagneux, Cabanes

and Domine[8]). In particular, for accurate low-SSA snow measurements, sampling should particularly take care of preserving the microstructural network. Using snow fragments or finest grains resulting from sieving would however correspond to measuring the sum SSA + SGCA, with SGCA being of the same order of SSA. The results presented in Figure 6 explain why sampling effects are particularly more sensitive on rounded grains, crusts and melt forms than on fresh snow.

From a more conceptual point of view, the SGCA is a parameter that provides scalar information on the bonding area between grains, data that is not available from the sole classical SSA. This could be an interesting parameter to relate with thermal or mechanical properties[12]. When associated with SSA, SGCA might also be an appropriate parameter to help in characterizing snow quantitatively (as permeability in the recent work of Arakawa et al.[25]). Developing experimental methods that can provide accurate SGCA values on the field seems a challenging, but promising approach.

4. SUMMARY

We applied diverse SSA numerical computations on a set of ten tomographic images corresponding to various snow types. The major results can be summarized as follows:

There is no ideal numerical method to estimate the SSA. The Voxel Projection (VP) method is particularly appropriate if the image details are described by a large number of voxels. Otherwise, the stereological method would be a reasonable alternative. The standard Marching Cubes algorithm always overestimates the SSA.

SSA measurements from tomographic images are particularly sensitive to the image resolution. As concluded in the work of Kerbrat et al.[5], a voxel size of 30 μm is generally sufficient to compute the SSA with reasonable accuracy. However, the snow type imaged as well as the method used may have a drastic impact on this estimation.

From the computed SSA estimations, the REV seems to be attained for an edge size of 2.5 mm.

Thanks to the combination of the VP method with the CDGS algorithm[5], it is possible to estimate the specific Grain Contact Area (SGCA). The use of this quantity shows that low-SSA samples can provide a large proportion of SSA after neck breaking, which may significantly impact SSA measurements. More generally, the SGCA seems an interesting parameter that may be particularly useful for snow microstructural characterization.

ACKNOWLEDGMENTS

The authors are particularly grateful to the scientists of the ESRF ID19 beamline (J. Baruchel, E. Boller, W. Ludwig, X. Thibault) and of the 3SR laboratory (P. Charrier, J. Desrues), where the 3D images have been obtained. We also would like to thank L. Arnaud, F. Domine, M. Kerbrat, G. Picard and M. Schneebeli for fruitful discussions.

REFERENCES

(1) E. E. Underwood, Quantitative Stereology, Addison-Welsey, Reading, Massachusetts.
(2) S. Torquato, Random Heterogeneous Materials: Microstructure and Macroscopic Properties, Springer-Verlag, New-York, 2002, p.47-48.
(3) W.E. Lorensen, H.E. Cline, *Computer Graphics*, **21**(4), 163-169 (1987).
(4) F. Flin, J.-B. Brzoska, D. Coeurjolly, R. A. Pieritz, B. Lesaffre, C. Coleou, P. Lamboley, O. Teytaud, G. L. Vignoles, J.-F. Delesse, *IEEE Trans. Image Process.*, **14**(5), 585-596 (2005).
(5) L. Gillibert, F. Flin, J. Kozicki, S. Rolland du Roscoat, W. Ludwig, D. Coeurjolly, B. Chareyre, A. Philip, B. Lesaffre, J. Meyssonnier, Proceedings of the 3rd International Workshop: 3D Imaging, Analysis, Modeling and Simulation of Macroscopic Properties, in press.
(6) H.-W. Jacobi, F. Domine, W. R. Simpson, T. A. Douglas, M. Sturm, *The Cryosphere*, 4, 35-51 (2010).
(7) J.-C. Gallet, F. Domine, C. Zender, G. Picard, *The Cryosphere*, **3**, 167-182 (2009).
(8) L. Legagneux, A. Cabanes, F. Domine, *J. Geophys. Res.,* **107**(D17), 4335, doi:10.1029/2001JD001016 (2002).
(9) F. Flin, J.-B Brzoska, B. Lesaffre, C. Coleou, R. A. Pieritz, *Ann. Glaciol.*, **38**, 39-44 (2004).
(10) M. Kerbrat, B. Pinzer, T. Huthwelker, H. W.

Gaeggeler, M. Ammann, M. Schneebeli, *Atmos. Chem. Phys.,* **8**, 1261-1275 (2008).
(11) M. Schneebeli, S.A. Sokratov, *Hydrol. Process.*, **18**, 3655-3665 (2004).
(12) K.F. Voitkovsky, A.N. Bozhinsky, V.N. Golubev, M.N. Laptev, A.A. Zhigulsky, Yu.Ye. Slesarenko, International symposium on snow mechanics, IAHS–AISH Publication vol. 114, Grindelwald, Switzerland, 1975, p.171–179.
(13) J.-B. Brzoska, F. Flin, N. Ogawa, Using Gaussian curvature for the 3D segmentation of snow grains from microtomographic data, in: W. Kuhs (Ed.), Physics and Chemistry of Ice, RSC Publishing, Cambridge, 2007, p.125-132.
(14) F. Flin, J.-B. Brzoska, *Ann. Glaciol.*, **49**, 17-21 (2008).
(15) L. Arnaud, G. Picard, N. Champollion, S. Morin, F. Domine, F. Flin, B. Lesaffre, A. Royer, A. Langlois. P. Cliche, D. Six, J-M. Barnola, M. Fily, poster presentation, International Snow Science Workshop, Davos (2009); http://www-lgge.obs.ujf-grenoble.fr/~picard/fichiers/poster-issw2009.pdf
(16) C.F. Raymond, K.T. Tusima, *J. Glaciol.*, **22**(86), 83-105 (1979).
(17) C. Fierz, R.L. Armstrong, Y. Durand, P. Etchevers, E. Greene, D.M. McClung, K. Nishimura, P.K. Satyawali, S.A Sokratov, The International Classification for Seasonal Snow on the Ground, IHP-VII Technical Documents in Hydrology N°83, IACS Contribution N°1, UNESCO-IHP, Paris, 2009, p.13-20.
(18) J.-B. Brzoska, F. Flin, B. Lesaffre, C. Coleou, P. Lamboley, J. F. Delesse, B. Le Saec, G. Vignoles, Image Anal. Stereol., **20**(suppl. 1), 306-312 (2001).
(19) D. Coeurjolly, F. Flin, O. Teytaud, L. Tougne, Multigrid convergence and surface area estimation, in T. Asano, R. Klette, C. Ronse, (Eds.), 11th International Workshop on Theoretical Foundations of Computer Vision: Geometry, Morphology, and Computational Imaging, Springer-Verlag, vol. 2616 of Lecture Notes in Computer Science, 2003, p.101-119.
(20) W. Ludwig, P. Reischig, A. King, M. Herbig, E.M. Lauridsen, G. Johnson, T.J. Marrow, J.Y. Buffiere, *Review of Scientific Instruments*, **80**(3), 033905 (2009); doi:10.1063/1.3100200
(21) S. Rolland du Roscoat, A. King, A. Philip, P. Reischig, W. Ludwig, F. Flin, J. Meyssonnier, *Adv. Eng. Mater.*, in press.
(22) R. Glantz, M. Hilpert, *Advances in Water Resources*, **31**, 787-806 (2008).
(23) M.W. Hoerhold, M.R. Albert, J. Freitag, *J. Glaciol.*, **55**(192), 625-630 (2009).
(24) M. Matzl, M. Schneebeli, *Cold Reg. Sci. Technol.*, in press; doi:10.1016/j.coldregions.2010.06.006.
(25) H. Arakawa, K. Izumi, K. Kawashima, T. Kawamura, *Cold. Reg. Sci. Technol.*, **59**, 163-168 (2009).